Arrangement of Core Membrane Segments in the MotA/MotB Proton-Channel Complex of *Escherichia coli*†

Timothy F. Braun, Laith Q. Al-Mawsawi, Seiji Kojima, and David F. Blair*

Department of Biology, University of Utah, Salt Lake City, Utah 84112

Received August 6, 2003; Revised Manuscript Received October 22, 2003

ABSTRACT: The stator of the bacterial flagellar motor is formed from the membrane proteins MotA and MotB, which associate in complexes with stoichiometry $MotA_4MotB_2$ (Kojima, S., and Blair, D. F., preceding paper in this issue). The MotA/MotB complexes conduct ions across the membrane, and couple ion flow to flagellar rotation by a mechanism that appears to involve conformational changes within the complex. MotA has four membrane-crossing segments, termed A1−A4, and MotB has one, termed B. We are studying the organization of the 18 membrane segments in the $MotA_4MotB_2$ complex by using targeted disulfide cross-linking. A previous cross-linking study showed that the two B segments in the complex (one from each MotB subunit) are arranged as a symmetrical dimer of α-helices. Here, we extend the cross-linking study to segments A3 and A4. Single Cys residues were introduced by mutation in several consecutive positions in segments A3 and A4, and double mutants were made by pairwise combination of subsets of the Cys replacements in segments A3, A4, and B. Disulfide cross-linking of the single- and double-Cys proteins was studied in whole cells, in membranes, and in detergent solution. Several combinations of Cys residues in segments A3 and B gave a high yield of disulfide-linked MotA/MotB heterodimer upon oxidation with iodine. Positions of efficient cross-linking identify a helix face on segment A3 that is in proximity to segment(s) B. Some combinations of Cys residues in segments A4 and B also gave a significant yield of disulfide-linked heterodimer, indicating that segment A4 is also near segment(s) B. Certain combinations of Cys residues in segments A3 and A4 cross-linked to form MotA tetramers in high yield upon oxidation. The high-yield positions identify faces on A3 and A4 that are at an interface between MotA subunits. Taken together with mutational studies and patterns of amino acid conservation, the cross-linking results delineate the overall arrangement of 10 membrane segments in the MotA/MotB complex, and identify helix faces likely to line the proton channels.

The stator of the bacterial flagellar motor is formed from the membrane proteins MotA and MotB, which form complexes with composition $MotA_4MotB_2$ (*1*). The MotA/MotB complexes conduct protons across the membrane, and couple proton flow to rotation by a mechanism that appears to involve a conformational powerstroke driven by protonation/deprotonation of an invariant Asp residue, Asp32, in MotB (*1*, *2*). The mechanisms of proton movement and force generation are not yet understood in detail, mainly owing to a lack of structural information on the MotA/MotB complex.

Figure 1 illustrates the membrane topologies of the Mot proteins, and some features that were found by mutational analysis to be important for function. MotA has four membrane segments, sizable domains in the cytoplasm, and only short loops in the periplasm (*3*, *4*). The MotA cytoplasmic domain contains two charged residues that are quite important for motor rotation in *E. coli*, Arg90 and Glu98, and a third that is somewhat important, Arg150. These three charged residues of MotA interact with charged residues of the rotor protein FliG (*5*, *6*). Two Pro residues near the inner ends of segments A3 and A4 are conserved and important for function. These might regulate the conformation of the complex, and/or conformational changes (*7*). MotB has a short segment in the cytoplasm, a single membrane segment, and a large domain in the periplasm (*8*, *9*). The periplasmic domain of MotB includes a sequence motif found in proteins that bind peptidoglycan (*10*), and is presumed to form an attachment to the cell wall. The putative proton-transferring residue Asp32 is near the inner end of the MotB membrane segment.

As shown in the preceding paper in this issue, MotA/MotB complexes can be solubilized and purified, and retain important conformational properties of the proteins in membranes provided an appropriate detergent is used. We have not yet succeeded in crystallizing the complex for X-ray structural studies. As an alternative means of obtaining some structural information, we are undertaking targeted disulfide cross-linking studies on the membrane segments of the complex. The complex is predicted to have 18 membrane segments in all, 16 contributed by the MotA subunits and 2 from the MotB subunits (Figure 1). The disulfide cross-linking approach has been shown to be useful for determining general features of membrane-segment arrangement in bacte-

† Supported by Grant 1-R01-GM64664 from the U.S. National Institutes of Health (to D.F.B.) and a postdoctoral fellowship from the Japan Society for the Promotion of Science (to S.K.). T.F.B. received partial support from NIH Training Grant 5T32-GM08537. The Protein-DNA core facility at the University of Utah receives support from the National Cancer Institute (Grant 5P30 CA42014).

* To whom correspondence should be addressed. Phone: (801) 585-3709. Fax: (801) 581-4668. E-mail: blair@bioscience.utah.edu.

10.1021/bi035406d CCC: $27.50
Published on Web 12/16/2003

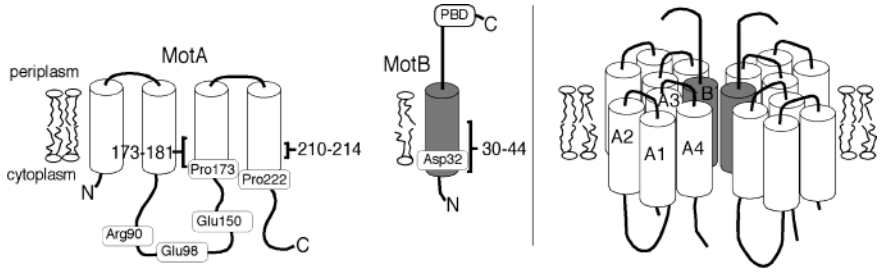

FIGURE 1: (Left) Membrane topologies of the MotA and MotB proteins, and features found to be important for function in mutational studies. Functions of specific residues are discussed in the text. Topologies are based on refs *3*, *4*, *8*, and *9*. Brackets indicate the parts of segments A3, A4, and B where cysteine replacements were made for this cross-linking study. PBD = peptidoglycan binding domain. (Right) Hypothetical arrangement of subunits in the $MotA_4MotB_2$ complex. The subunit composition is based on data in the preceding paper in this issue (*1*) and ref *24*. The central position of the MotB dimer is suggested by cross-linking data in ref *18*. The arrangement of the 16 MotA segments is not known, but mutational data (*7*, *21*−*23*) suggest inward locations for segments A3 and A4, as pictured.

rial chemoreceptors (*11*, *12*) and a number of other membrane proteins (e.g., refs *13*−*17*).

In a previous cross-linking study, we showed that the membrane segments of the two MotB subunits are in close contact. A high yield of disulfide cross-linked MotB dimer was observed for Cys replacements spaced at regular intervals of 3−4 residues, as expected for a symmetrical dimer of α-helices (*18*). The cross-linking results indicate that the B segments interact along equivalent faces, so the $MotA_4MotB_2$ complex could have 2-fold symmetry about an axis perpendicular to the membrane and centered on the B−B subunit interface. The four MotA subunits would then be arranged around the MotB dimer. The MotA subunits must occupy at least two nonequivalent environments, given that the complex can have no higher than 2-fold symmetry.

Here, we describe disulfide cross-linking studies involving membrane segments A3, A4, and B. Cys replacements in segment B were made for the previous cross-linking study (*18*); for the present study single Cys residues were introduced in several positions in segments A3 and A4. Subsets of the single-Cys mutations were combined to give double mutants with pairs of Cys residues in various places in segments A3, A4, and B. Disulfide cross-linking was studied in cells, membranes, and detergent solution, using anti-MotA and anti-MotB immunoblots to analyze the products. The observed patterns of cross-linking are consistent with an arrangement in which the central dimer of MotB segments is surrounded by the A3 and A4 segments of four MotA subunits. The cross-linking results, together with patterns of residue conservation and results from mutational studies, support a specific model for the arrangement of 10 membrane segments in the core of the MotA/MotB complex.

EXPERIMENTAL PROCEDURES

Strains, Plasmids, and Mutagenesis. Cys-replacement mutations in segments A3 and A4 were made by using the altered sites procedure (Promega), in plasmid pRF5, a derivative of pAlter-1 that encodes *motA* and *motB*. The *motA* gene in pRF5 contains a mutation that replaces the only native Cys (residue 240) with Ser, which was shown to have only a minor effect on swarming rates in soft-agar plates (*18*). Cys replacements in MotB were also made in pRF5; their construction and assays of their function were reported previously (*18*). For most cross-linking experiments, proteins were expressed in strain BL21(De3) (*19*), not induced, giving moderate overexpression of MotA and MotB (ca. 10-fold wild type). The function of mutant MotA proteins, and MotA/MotB double mutants, was assayed by expressing the proteins in the *motAB*-deletion strain RP6894, a gift from J. S. Parkinson (University of Utah). In this host, the plasmids give MotA and MotB levels comparable to those of the wild type.

Double mutations with Cys replacements in segments B and A3 were constructed by transferring an *Mlu*I−*Nsi*I restriction fragment containing the segment B mutation into a similarly digested vector containing the segment A3 mutation. Segment A3/A4 double mutations were constructed in the same way, except the restriction fragments contained the segment A4 mutations. To construct the A4/B double mutations, the A4 mutations were first transferred into plasmid pTB36. pTB36 encodes *motA* and *motB* behind the T7 promoter, and gives expression levels similar to pRF5, but is deleted for an interfering *Sap*I site present in pRF5. The pTB36 plasmids encoding the A4 mutations were digested with *Sap*I, and then a 350-bp *Sap*I restriction fragment of pRF5 containing the segment B mutations was inserted. Three of the A4/B double mutations (210/41, 210/40, and 210/38) were made directly by using two mutagenic oligonucleotides. All mutations and ligation steps were confirmed by DNA sequencing. Sequencing and oligonucleotide synthesis were performed by core facilities at the University of Utah. Plasmids were isolated using the QIAprep miniprep system (Qiagen).

Measurements of Swarming Motility. Rates of swarming in soft agar were measured as described previously (*7*), using RP6894 cells expressing the mutant proteins from plasmids (mutant variants of either pRF5 or pTB36, as noted above). Cells were spotted onto tryptone plates containing 0.28% agar, and swarm diameters were measured at regular intervals, usually once per hour. The rates reported are relative to the average of those of several wild-type controls spotted on a subset of the same plates.

SDS−PAGE and Immunoblotting. Protein samples were electrophoresed on nonreducing SDS−PAGE[1] minigels (Bio-Rad MiniProtein II system). Acrylamide concentrations were 7.5% for MotB blots and 8.5% for MotA blots. Proteins were transferred from gels onto nitrocellulose paper using a

[1] Abbreviations: CHAPS, 3-[(3-cholamidopropyl)dimethylammonio]-1-propanesulfonate; BME, β-mercaptoethanol; DPC, dodecylphosphocholine; EDTA, ethylenediaminetetraacetic acid; NEM, *N*-ethylmaleimide; SDS, sodium dodecyl sulfate; PAGE, polyacrylamide gel electrophoresis; Tris, tris(hydroxymethyl)aminomethane.

semidry transfer apparatus (Bio-Rad Transblot SD) for 30 min. Rabbit polyclonal anti-MotB antibody was prepared as described before (*20*), and was used at a dilution of 1/1250 in a 3% milk/TBS solution, pH 8. Polyclonal antibody against the larger cytoplasmic domain of MotA (residues 48−174) was obtained as described previously (*7*), and was used at a dilution of 1/1100 in a 4% milk/TBS solution containing 0.2% Tween-20 (Sigma). HRP-conjugated secondary antibody (Pierce Biotechnology) was used at a dilution of 1/12000 for MotB blots, and 1/48000 for MotA blots. Band intensities were quantified using a video densitometer and the software package NIH-Image.

Oxidative Cross-Linking. Most cross-linking experiments were performed on whole cells of strain BL21(De3) expressing the Cys-mutant Mot proteins from a plasmid. Cells were grown overnight at 37 °C with aeration in 2 mL of LB broth containing 100 μg/mL ampicillin. The final OD_{600} was typically about 2. Cells were collected by centrifugation and resuspended in 50 mM Tris, pH 8.0, 20 mM EDTA, to a volume giving an OD_{600} of 10. Two 100 μL aliquots were taken from each sample, one for oxidative cross-linking by iodine and one for use as a nonoxidized control.

Crystalline iodine (Sigma) was dissolved in 95% ethanol to make a 500 mM stock solution which was stored at −20 °C; experiments used a 200 mM working solution in 95% ethanol. Cross-linking experiments were conducted at room temperature. Samples were treated with 2 mM iodine for 2−3 min and then quenched with 20 mM NEM (Sigma) for 2−3 min. The NEM was added from a 1 M stock, prepared in 95% ethanol and stored at −20 °C. Samples were denatured by addition of SDS to 5%, followed by heating to 95 °C for 3−5 min. Nonoxidized control samples were exposed to just NEM (20 mM, 2−3 min) and then denatured as above. Cross-linking experiments with detergent-solubilized proteins followed the same procedure, except the iodine concentration was decreased, typically to 100 μM. Experiments to examine BME reduction of disulfide bonds used the iodine treatment described above, followed by treatment with 5% BME for 2−3 min and then quenching with NEM. Samples were either frozen for later use or prepared for SDS−PAGE by adding 1/9.5 volume of 10× loading buffer (35% glycerol, 8.5% sucrose, 7% SDS, 0.5 M Tris, pH 6.8, and 0.05% bromophenol blue).

Detergent Solubilization of MotA/MotB Complexes. Cells from a freezer stock were used to inoculate 30 mL of LB broth containing 100 μg/mL ampicillin, and grown overnight (typically 16 h) at 37 °C with aeration. The cells were collected by centrifugation (5000*g*, 10 min), and resuspended in 650 μL of buffer A (50 mM Tris, pH 8.0, 50 mM NaCl, 2 mM EDTA). Lysozyme (100 μL of a 6 mg/mL solution; hen egg white, Sigma) and EDTA (20 μL of 1 M stock) were added, and then the mixture was transferred to a microfuge tube and put on ice for 30 min. Samples were frozen at −70 °C, thawed, and then lysed by two rounds of sonication (90 and 60 s, Branson model 450 sonifier, power level 3, 50% duty cycle, ice temperature). Unlysed cells were pelleted by centrifugation (5000*g*, 8 min), and the supernatant was transferred to a fresh microfuge tube. Membranes were pelleted (14000*g*, 30 min) and resuspended in 300 μL of buffer A. Freshly prepared membrane samples were solubilized with CHAPS (Sigma), by adding an equal volume of 5% CHAPS, diluting the solution 10-fold into buffer A, and gently mixing for 1 h at 4 °C. Samples were spun (14000*g*, 15 min) to remove unsolubilized material. The supernatant containing detergent-solubilized proteins was used for cross-linking experiments, as detailed below. Some later solubilization experiments used the detergent DPC instead, which was found to be better than CHAPS for maintaining the stability of the complexes (*1*). Membranes were prepared as above, except that 200 μL of the membrane suspension was spun (14000*g*, 30 min), resuspended in 100 μL of 20 mM Tris−Cl, pH 8, 300 mM NaCl, 5 mM imidazole, 20% (w/v) glucose, and 0.05% DPC, and then incubated on ice for 10 min. The solution was mixed with 400 μL of the same buffer except with 20% glycerol in place of the glucose, and then the mixture was placed on ice for 10 min more. Insoluble material was removed by centrifugation (14000*g*, 10 min), and the supernatant was collected for cross-linking experiments.

For cross-linking experiments with solubilized proteins, 100 μL of the supernatant was mixed with ∼1 μL of 20 mM I_2 (final concentration 200 μM), incubated at room temperature for 90 s, and then quenched with NEM (2 μL of a 1 M stock, final concentration ca. 20 mM). Nonoxidized controls were treated with just the NEM. Samples were denatured by adding 50 μL of 10% SDS and boiling, electrophoresed on 8.5% gels, and examined on anti-MotA immunoblots using the protocols above.

MotA and MotB Sequences. Sequences of *motA* and *motB* genes were obtained from the website of the National Center for Biotechnology Information (www.ncbi.nlm.nih.gov). Some species contain two or more *motA* and *motB* genes, both or all of which were included in the alignment. The 39 sequences used in the alignment were from *Aquifex aeolicus*, *Bacillus halodurans*, *Bacillus subtilis* (2 sequences), *Bacillus megaterium*, *Clostridium acetobutylicum* (2 sequences), *Clostridium difficile* (2 sequences), *Carboxdothermus hydrogenoformans*, *Desulfitobacterium hafniense*, *Listeria monocytogenes*, *Caulobacter crescentus*, *Brucella suis*, *Rhodopseudomonas palustris*, *Rhizobium meliloti*, *Magnetospirillum magnetotacticum*, *Bordetella pertussis*, *Burkholderia cepacia*, *Nitrosomonas europaea*, *Desulfovibrio vulgaris* (4 sequences), *Geobacter sulfurreducens*, *Camplyobacter jejuni*, *Helicobacter pylori*, *Escherichia coli*, *Yersinia pestis* (2 sequences), *Legionella pneumophila*, *Shewanella putrefasciens* (2 sequences), *Vibrio alginolyticus*, *Pseudomonas aeruginosa* (2 sequences), *Borrelia burgdorferi*, *Treponema pallidum*, and *Thermotoga maritima*.

RESULTS

Cys Mutants. The preceding paper in this issue (*1*) presents evidence that the complex contains four copies of MotA and two copies of MotB. A previous cross-linking study showed that the membrane segments of the two MotB subunits form a symmetric dimer, which could be at the center of the complex (*18*). Mutational studies suggest that segments A3 and A4 are more centrally located in the complex than segments A1 and A2; segments A3 and A4 gave a higher frequency of random mutations that impair rotation (*21*, *22*) and were less tolerant of replacements by tryptophan (*23*). Segments A3 and A4 also contain more invariant or well-conserved residues than segments A1 and A2. The present cross-linking experiments therefore focused on segments A3, A4, and B.

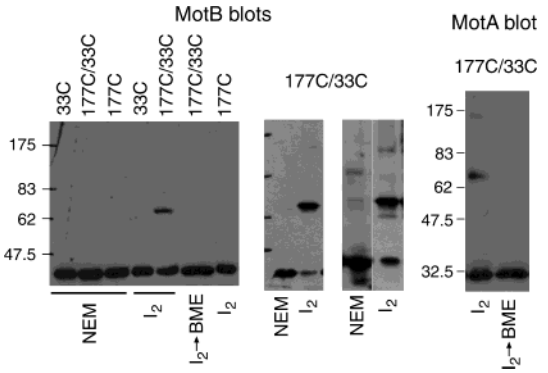

FIGURE 2: Disulfide cross-linking between Cys residues in MotA and MotB. Immunoblots used antibodies against MotA or MotB, as indicated. Cys replacements were in position 33 in segment B and/or position 177 in segment A3. Chemical treatments are indicated below the blots. The yield of MotA/MotB heterodimer was somewhat lower than usual on the left gel; additional examples showing the high yield typical of 177−33 cross-linking are shown in the middle.

Wild-type MotA contains one Cys, residue 240, that was mutated to Ser with little effect on function (*18*). Site-directed mutagenesis was used to introduce single Cys residues in 17 consecutive positions in segment A3 (residues 172−188) and 5 positions in segment A4 (residues 210−214). The approximate location of the Cys replacements within each membrane segment are indicated in Figure 1. A set of 68 A3/B double mutants was constructed by combining each of nine Cys replacements in segment A3 (positions 173−181) with six to nine Cys replacements in segment B. A set of 27 A3/A4 double mutants was constructed by combining each of the five Cys replacements in A4 with several replacements in A3. A set of 17 A4/B double mutants was constructed by combining each of four Cys replacements in A4 (210−213) with several Cys replacements in segment B.

The mutant proteins were expressed from a plasmid that has the *motA* and *motB* genes in their normal relationship, to retain the normal MotA:MotB ratio. Protein levels in the single- and double-Cys mutants were examined on immunoblots of whole-cell proteins from overnight cultures. In most of the mutants, proteins accumulated to levels comparable to those of the wild-type proteins expressed from the same plasmid. Three of the proteins with Cys replacements in A3 (174, 175, and 176) showed MotA levels that were lower than that of the wild type, but still detectable. Levels of both MotA and MotB were significantly decreased in some of the double mutants that combined a Cys in segment B with Cys 180 in segment A3 (not shown); these double mutants were not studied further.

Cross-Linking between Segments A3 and B. To study A3−B cross-linking, cells expressing the A3/B double-Cys-mutant proteins were exposed to I_2 (2 mM), and the products were analyzed on immunoblots, first using anti-MotB antibody. In many of the double-Cys mutants, oxidation with I_2 gave a band with an apparent mass of ~65 kDa, close to the position expected for a MotA/MotB heterodimer (Figure 2). Several of the mutants that gave a high yield of the putative A−B heterodimer were then examined on MotA immunoblots, and a 65 kDa band was again seen. The band was not seen or was greatly diminished in intensity in the single-Cys mutants, and was also eliminated or diminished when samples were treated with BME to reduce disulfide bonds. Together, these results show that the band is a disulfide-linked MotA/MotB heterodimer.

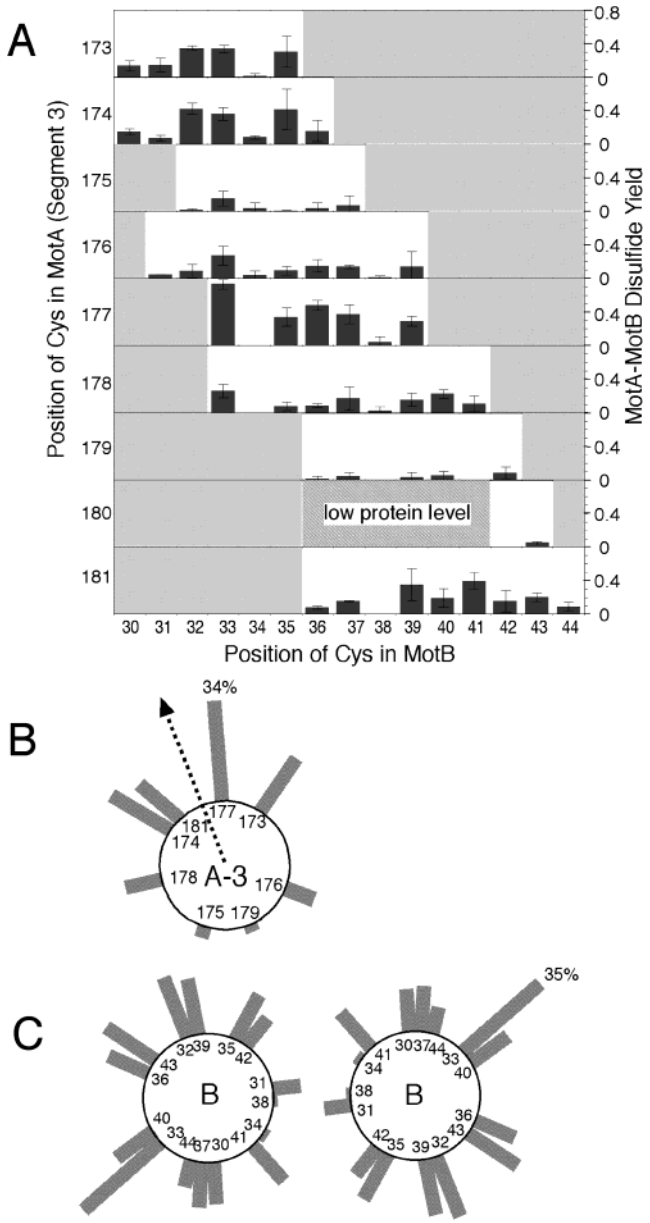

FIGURE 3: (A) Summary of yields of A3−B disulfide cross-linking, for all A3/B double mutants. Products of A3−B cross-linking were quantified on anti-MotB immunoblots, and are given relative to the total amount of MotB present. The values plotted are averages of three determinations, ±sd. (B) Average yields for disulfide cross-linking of each position in segment A3 to all of its tested partners in segment B. Average yields are represented by bars, positioned on an α-helical projection of the segment. The dashed arrow is the A3-to-B cross-linking moment obtained by vector addition of the bars. (C) Average yields for disulfide cross-linking of each position in segment B to all tested partners in segment A3. Data are presented in the same way as in panel B, except that a dimer of MotB segments is shown, arranged according to the results from a cross-linking study of MotB (*18*).

The A/B heterodimer band was quantified on MotB immunoblots, and the yield of A/B heterodimer was calculated relative to the total MotB present. Yields for all of the A3/B double mutants are summarized in Figure 3. The A3−B cross-link yields depended on the positions of both Cys residues, and ranged from 0 to more than 70%. To see overall

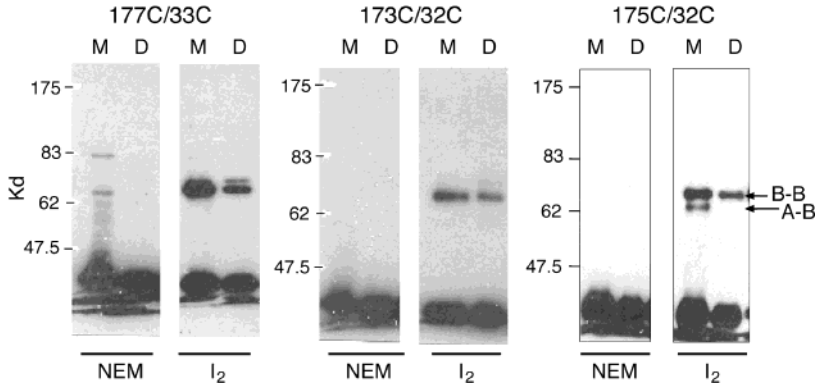

FIGURE 4: Cross-linking between segments A3 and B in detergent-solubilized samples. (Left and middle) Results with two double mutants that gave a relatively high cross-link yield in membranes. Samples were either isolated membranes (M) or membranes solubilized with the detergent CHAPS (0.5%) for 1 h (D). Nonoxidized controls were treated with only NEM, and experimental samples with iodine, followed by NEM. (Right) Results with the 175/32 double mutant, which gave a lower yield of A3−B cross-linking in membranes. The upper band was also observed in the 32C single mutant (not shown), indicating that it is a MotB dimer, as labeled.

patterns of cross-linking, the average yields for cross-linking of each position to all of its tested partners are shown on helical projections of the membrane segments in Figure 3 (panels B and C). Two MotB segments are shown, arranged according to the results of the previous cross-linking study (*18*). Several positions around the outside of the B dimer cross-linked to segment A3 in moderate yield (12−35%; average yield 18%). By contrast, the three positions nearest the B−B subunit interface (31, 34, and 38) gave relatively low yields of cross-linking to A3 (average yield 4%). In segment A3, positions that cross-linked to B in high yield were 173, 174, 177, and 181, which should lie on one face of a helix. For segment A3, the position-averaged cross-linking yields were added vectorially to give a "cross-linking moment", which points in a direction between residues 177 and 181 (Figure 3B).

To verify that cross-linking occurred within a preexisting complex rather than by collision of separate molecules in the membrane, cross-linking experiments were done on selected A3/B double mutants solubilized in CHAPS (0.5%). Two double mutants that gave a good yield of A/B heterodimer in membranes (A173/B32 and A177/B33) also gave a significant yield in CHAPS solution (Figure 4), indicating that cross-linking between A3 and B can occur within detergent-solubilized complexes. Several double mutants that gave a low heterodimer yield in membranes (A175/B32, A175/B33, A175/B35, and A179/ B36) gave a negligible yield in CHAPS solution (A175/B32 example shown in Figure 4). Some or all of the low-yield cross-linking may thus occur through collision.

The complex contains multiple, probably four, copies of MotA (*1*), which might account for the ability of so many positions around the segment B dimer to cross-link to A3 (Figure 3C). In a complex with multiple MotA subunits, the A3 segments of different subunits might also cross-link to each other. This was tested by expressing MotA proteins with single-Cys replacements in A3 along with Cys-less (wild-type) MotB, treating the cells with I_2 (2−5 mM), and examining the products on anti-MotA blots. Most of the A3 Cys mutants exhibited little or no cross-linking. In three of the A3 Cys mutants (positions 175, 176, and 187), I_2 treatment gave a significant band at the position expected for the MotA dimer, but this product was eliminated when

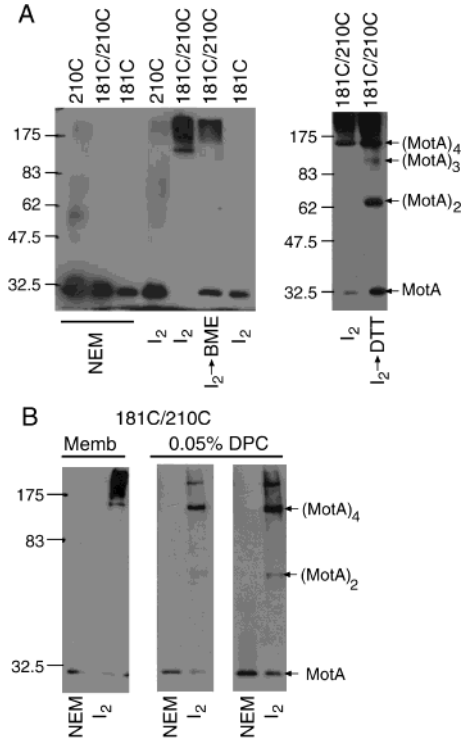

FIGURE 5: (A) MotA multimers formed by cross-linking of the 181/210 double-Cys mutant. The blots used anti-MotA antibody. Cys replacements are indicated above the lanes, and chemical treatments below. (B) Persistence of the cross-linked tetramer, and loss of most higher molecular weight products, in a cross-linking experiment with complexes solubilized in detergent. The blots used anti-MotA antibody. Cross-linking was done in membranes or in 0.05% DPC, as indicated. For the experiment with detergent-solubilized proteins, two exposures of the same gel are shown; the longer exposure is to reveal the MotA dimer band.

samples were solubilized in CHAPS before oxidation, or if the proteins were expressed at lower levels (data not shown). Thus, while some A3−A3 cross-linking can occur, it appears to be through collision rather than in a preexisting complex. The absence of strong A3−A3 cross-linking indicates that the A3 segments of different MotA subunits in the complex are probably not in direct contact.

Intersubunit Cross-Linking between Segments A3 and A4. To study cross-linking between segments A3 and A4, cells

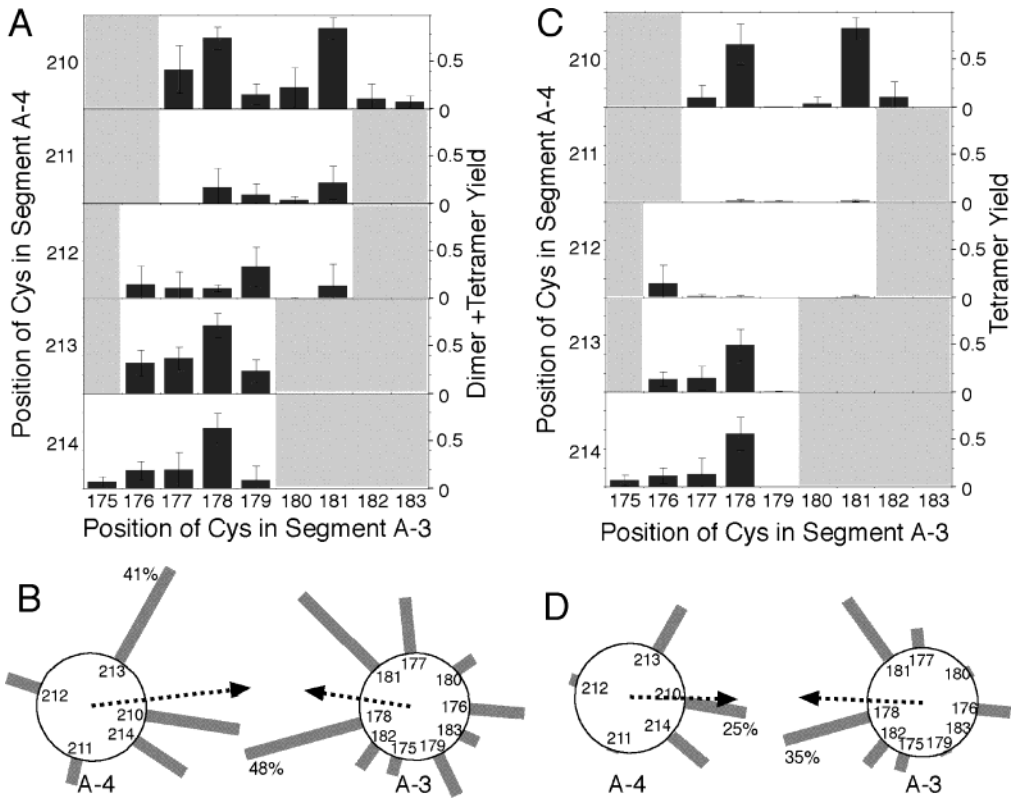

FIGURE 6: Summary of yields of A3−A4 disulfide cross-linking. Cross-linked products were quantified on anti-MotA immunoblots. (A) Yields of the dimer + tetramer, relative to the total MotA present in the monomer + dimer + tetramer. Values are averages for three determinations, ±sd. (B) Average yields of the dimer + tetramer, for cross-linking of each position in segment A3 to all tested partners in segment A4, and of each position in A4 to all tested partners in A3. Bars represent the average yield for each position. The dashed arrows are vector sums of the bars. (C) As in panel A, except yields are of the tetramer only, relative to the total amount of MotA in the tetramer + dimer + monomer. (D) Average yields of the tetramer, for cross-linking of each position in segment A3 to all tested partners in A4, and for cross-linking of each position in A4 to all tested partners in A3.

expressing the A3/A4 double-mutant proteins were exposed to I_2 (2 mM), and products were examined on anti-MotA blots. Several of the A3/A4 double mutants gave a band at the position expected for a MotA dimer, which was detected on MotA immunoblots but not MotB immunoblots and required the presence of both Cys residues (not shown). Certain of the A3/A4 double mutants also gave a high yield of larger cross-linked products, which included a band at about the position expected for a MotA tetramer, as well as products at higher molecular weight. An example is shown in Figure 5. The larger cross-linked products were seen on MotA blots but not MotB blots, and required the Cys replacements in both A3 and A4. Thus, they appear to be, or to contain, multimers of MotA. All of the putative tetramer, and most of the higher molecular weight material, was eliminated by BME treatment, indicating that it is cross-linked by disulfide bonds (Figure 5). A portion of the higher mass material was not eliminated by BME and could be cross-linked by different chemistry or aggregated into a form resistant to reduction. When the cross-linked material was treated with DTT instead of BME, the reduction to monomer was less complete and a strong band was seen at the MotA dimer position, as well as a weaker band at about the position expected for a trimer (Figure 5).

To see if the material larger than a tetramer arose by collisional cross-linking between separate stator complexes, cross-linking experiments were done in detergent solution (0.05% DPC), with two of the A3/A4 double mutants (178/210 and 181/210) that gave a high yield of tetramer and higher MW products in membranes. Results were similar for the two double mutants; data for 181/210 are shown in Figure 5. The tetramer was still produced in good yield in detergent solution, indicating that it is formed by cross-linking within a stable complex. The higher molecular weight bands were almost eliminated, as expected if they are products of collisional cross-linking.

Yields of cross-linked tetramer, and of cross-linked tetramer plus dimer, were measured for all of the A3/A4 double mutants. The results are summarized in Figure 6. Position-averaged yields were calculated and are shown on helical projections of the segments. In both A3 and A4, positions that give high tetramer yield occur on particular helix faces, defined by residues 178 and 181 in A3, and residues 210, 213, and 214 in A4. These faces on A3 and A4 are evidently in close contact at a MotA−MotA subunit interface. In segment A3, the surface that cross-links efficiently to A4 is distinct from that which cross-links efficiently to MotB (compare Figures 3 and 6).

Cross-Linking between Segments A4 and B. To study cross-linking between segments A4 and B, cells expressing the A4/B double-mutant proteins were treated with I_2 (2 mM), and products were examined on anti-MotB immunoblots. Certain of the A4/B double-Cys mutants gave a fair yield of a band near the position expected for a MotA/MotB heterodimer. Two examples (A210/B40 and A210/B41) are shown in Figure 7. The band was not seen, or was much

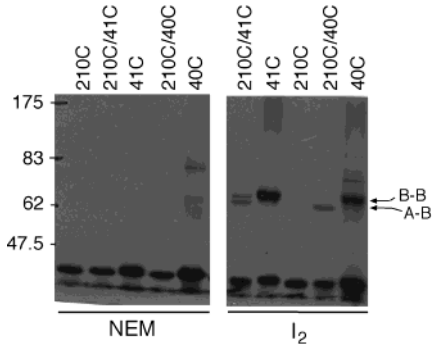

FIGURE 7: Examples of disulfide cross-linking between Cys residues in A4 and B. Positions of Cys replacements are indicated at the top; 40 and 41 refer to MotB and 210 to MotA. The blots used anti-MotB antibody.

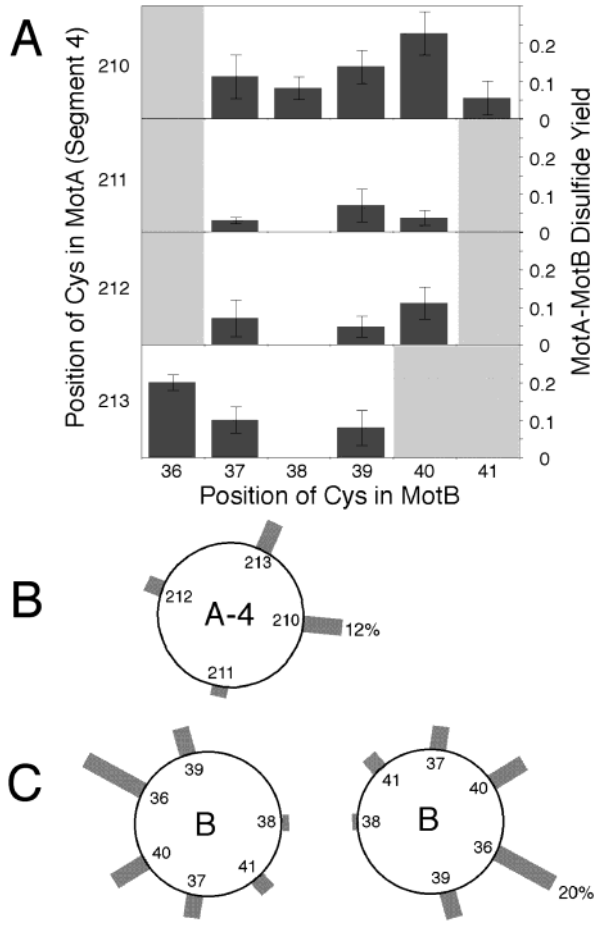

FIGURE 8: (A) Summary of yields of A4−B disulfide cross-linking. The intensities of A4−B product bands were measured on anti-MotB immunoblots. Yields are relative to the total MotB present. Values are averages for three determinations, ±sd. (B) Average yields for cross-linking of each position in segment A4 to all of its tested partners in segment B. (C) Average yields for cross-linking of each position in segment B to all tested partners in segment A4.

less intense, in the single-Cys mutants, and was eliminated by treatment with BME. It thus appears to be a disulfide-linked MotA/MotB heterodimer.

Yields of A4−B cross-linking for all the positions tested are summarized in Figure 8. The A4−B cross-linking yields depended on the positions of both Cys replacements, and ranged from 0 to 23%, about one-third the typical A3−B yields. Thus, segment A4 is within cross-linking distance of segment B, but appears less close than segment A3. Average yields for cross-linking of each position to all of its tested partners were computed, and are displayed on helical projections of the A4 and B segments. As with A3−B cross-linking, A4−B cross-linking occurred in fair yield (7−20%) for several positions around the outside of the B dimer, and the yields were lower when the Cys in segment B was near the B−B interface (at positions 38 or 41). In segment A4, positions 210 and 213 gave a somewhat higher yield than positions 211 and 212, but the pattern was not clear enough to identify a particular face likely to point toward segment B.

Function of the Cys-Replacement Mutants. The function of the single- and double-Cys mutants was assayed by expressing them in a *motAB*-deletion strain and measuring the rates of swarming in soft-agar tryptone plates. Swarming requires rapid rotation of the flagella, and so provides a sensitive assay of motor function. Function of the segment B Cys-replacement mutants was reported previously (*18*); all except the replacement of Asp32 permitted cells to swarm. Most of the Cys replacements in A3 or A4 also permitted swarming in soft agar. Exceptions were the replacement of residue 212 in A4, an invariant Gly, and replacements at three consecutive positions near the inner end of segment A3 (residues 174−176), a region that was found to be important for function in previous mutational studies (*7*, *21*, *22*). The 212, 174, 175, and 176 mutants did not swarm in soft agar, and in liquid culture the cells were immotile.

The function of the double-Cys mutants was also measured by the swarming assay, and the results are summarized in Figure 9. More than half of the A3/B double mutants functioned more poorly than expected for purely additive defects (Figure 9A). Synergistic defects occurred most frequently with residues 173 and 177 in A3, which also gave the highest efficiency cross-linking to MotB (Figure 3). One instance of suppression was seen; the MotA mutation A174C eliminated swarming when MotB was the wild type, but allowed swarming at almost half the normal rate when MotB had the mutation A36C. In the A3/A4 double mutants, instances of strong synergism were also seen but were less frequent than with the A3/B double mutants (5 double mutants were immotile, out of 18 combinations of motile single mutations). In the A4/B double mutants, swarming defects were approximately additive in most cases, with only two double mutants (210/38 and 210/41) functioning significantly more poorly than expected for purely additive defects.

DISCUSSION

Evidence for a stator complex containing more than one A and one B subunit was first reported by Sato and Homma (*24*) for the PomA/PomB proteins of the sodium-powered polar flagellum of *Vibrio*. A size estimate from gel filtration combined with an estimate of the A:B ratio from Coomassie-stained gels supported the subunit composition $PomA_4PomB_2$. The disulfide cross-linking results provide additional evidence for the subunit composition $MotA_4MotB_2$ in the *E. coli* proton-powered motor: MotA cross-links to form tetramers in good yield, even in detergent solution (Figure 7), and MotB cross-links to form dimers (*18*). Studies in the preceding paper in this issue also indicate a $MotA_4$-$MotB_2$ subunit composition, for the complex solubilized in the detergent dodecylphosphocholine (*1*).

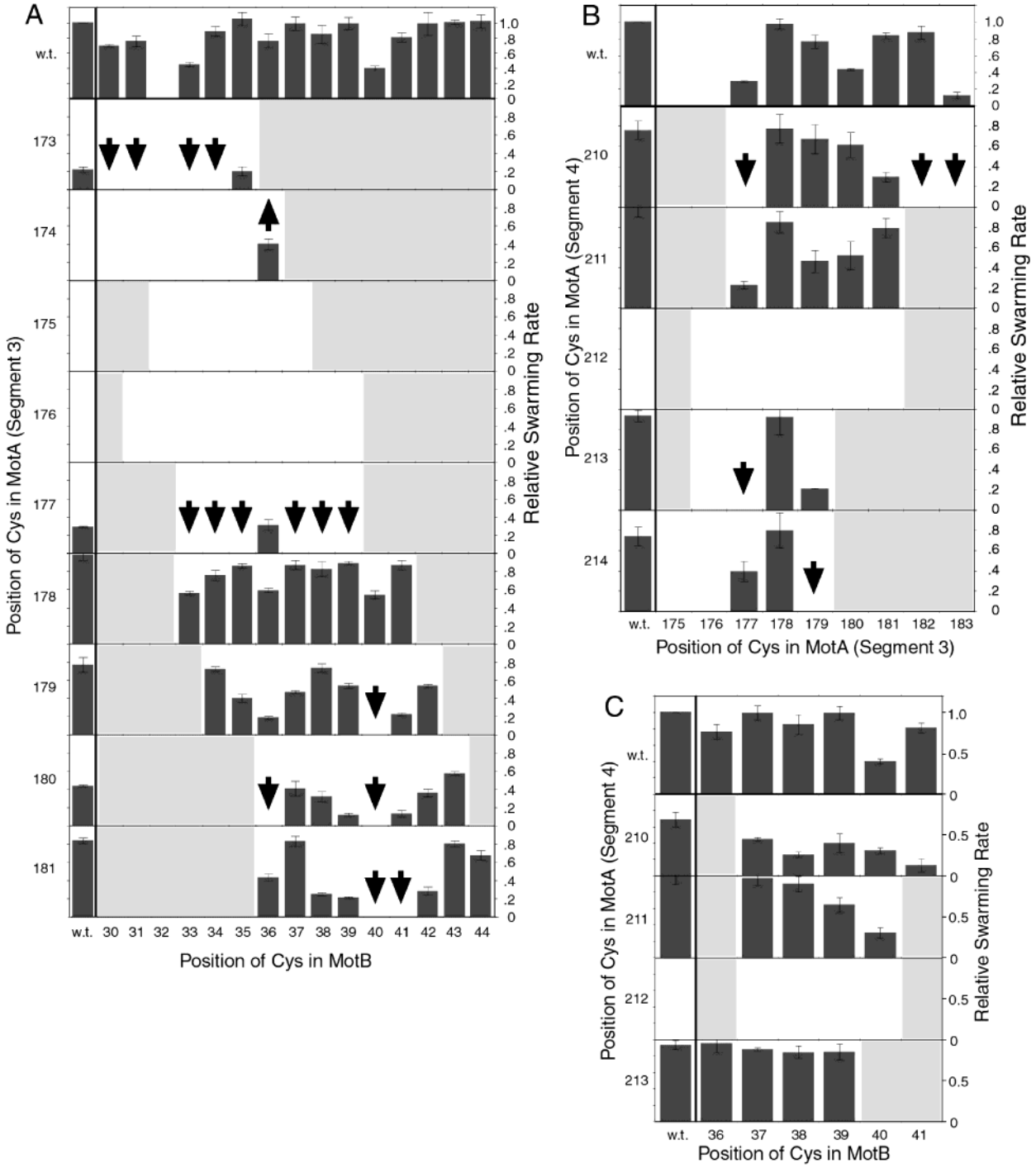

FIGURE 9: Swarming rates of the Cys mutants. Values are relative to those of wild-type controls measured in the same experiments, and are averages of three determinations, ±sd. (A) Mutants with Cys replacements in segment A3 and/or segment B. Data for the single-Cys MotB mutants are from ref *18*. Downward arrows indicate double mutants that showed a strong synergistic defect, failing to swarm even though the individual mutations permitted significant motility. The upward arrow is a double mutant that swarmed fairly well even though one of the individual mutations (174C) eliminated motility. (B) Mutants with Cys replacements in segments A3 and/or A4. Symbols are the same as in panel A. (C) Mutants with Cys replacements in segments A4 and/or B.

Given the subunit composition $MotA_4MotB_2$, the complex can have no greater than 2-fold symmetry, so the four MotA subunits must occur in at least two nonequivalent (i.e., not symmetry-related) environments. The high yield of cross-linked MotA tetramer seen in the 178/210 (or 181/210) double mutant implies that the contacts between adjacent pairs of MotA subunits must all be similar, however, in that residue 178 (and 181) of each MotA subunit must be near residue 210 of the adjacent one. Thus, although the four MotA subunits cannot be strictly equivalent, each one must be related to its neighbors (adjacent MotA subunits) in basically the same way.

The previous cross-linking study gave evidence for a symmetric dimer of MotB segments (*18*), and identified residues likely to form the B−B interface. Because segments A3 and A4 can both form disulfide cross-links to B, we suggest that the four MotA subunits in the complex are positioned with their A3 and A4 segments adjacent to the MotB dimer, and segments A1 and A2 in more outward positions. Patterns of high-yield cross-linking provide specific

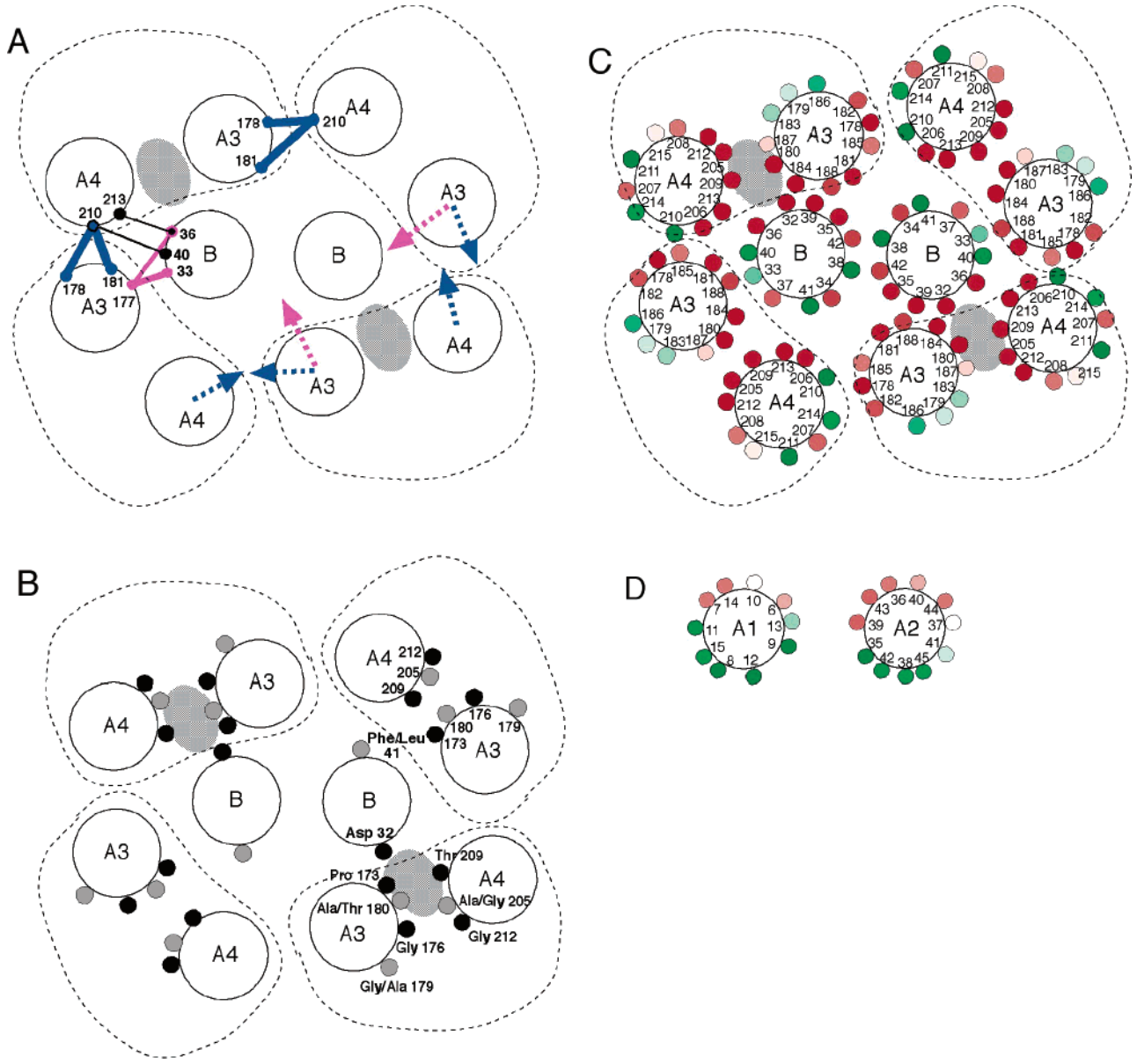

FIGURE 10: Model for the arrangement of segments B, A3, and A4 in the MotA/MotB complex. In all panels, the view is from the periplasmic side of the membrane. The model pertains to the inner (cytoplasm-proximal) parts of the membrane segments, which were the focus of the present cross-linking experiments (cf. Figure 1). In panels A−C, dashed lines are drawn around the A3 and A4 segments within a subunit. The complex is hypothesized to contain two proton channels, indicated by the crosshatched areas. (A) Summary of principal cross-linking results. In the upper and left-hand parts of the drawing, the two strongest intersegment cross-links of each type are indicated (A3−B, pink; A4−A3, blue; A4−B, black). In the bottom and right-hand parts of the drawing, the cross-linking moment vectors are shown. The arrow in segment A4 points in the direction of the most efficient cross-linking to A3 (cf. Figure 6); those in segment A3 point in the direction of the most efficient cross-linking to B (cf. Figure 3) or A4 (Figure 6). (B) Patterns of residue conservation. Invariant residues are indicated by black circles, and highly conserved positions (where only two different residues occur) by gray circles. The alignment used 39 MotA and MotB sequences, listed in the Experimental Methods. (C) Effects of Trp replacements in membrane segments B, A3, and A4. Data are from refs *23* and *25*. Some Trp-mutagenesis results on the outer part of the MotB segment are not shown, as they are away from the region studied here by cross-linking. Positions where Trp replacements permit motor function are colored green, with the intensity of color in proportion to the rate of swarming. Positions where Trp replacements eliminate function are colored red, with intensity of color in proportion to the dominance (the ability of the mutant protein to impair motility when expressed in wild-type cells). For measured values of the swarm rates and dominance, see refs *23* and *25*. (D) Summary of the effects of Trp replacements in A1 and A2, shown for comparison with the A3 and A4 results in panel C. About half of the positions in A1 and A2 tolerate Trp replacements, and most of the nonfunctional mutations are not strongly dominant.

constraints: the face on A3 defined by residues 173, 174, 177, and 181 must lie toward B, and the face on A3 defined by residues 178 and 181 must point toward A4 of an adjacent subunit. Segment A4 must be oriented so that residues 210, 213, and 214 are toward the interface with A3. An arrangement of segments that satisfies these constraints is shown in Figure 10.

Because most positions around the B dimer were found to cross-link to A3 (or A4) with comparable efficiencies, the cross-linking data alone cannot precisely locate segments A3 and A4 relative to Asp32 or any other landmarks on the B segments. The particular arrangement shown in Figure 10 is based on additional information as well, mainly patterns of sequence conservation in MotA and MotB homologues

from diverse species. Figure 10B shows residues in the segments that are invariant (only one amino acid found there in an alignment of 39 sequences) or well conserved (either one of two chemically similar amino acids found). In MotB, only the critical Asp residue is invariant, and just one other position (residue 41) is well conserved. Segments A3 and A4 have, between them, four invariant positions and three well-conserved positions. (Segments A1 and A2 are not pictured, but between them have no invariant residues and only one well-conserved residue.) In segments A3 and A4, the well-conserved positions are on helix faces predicted to point toward the interior of the subunit, roughly opposite the faces that gave efficient intersubunit cross-linking. We therefore suggest that the channel lies between the A3 and A4 segments of a MotA subunit, rather than at the interface between subunits. Accordingly, the A3 and A4 segments of a MotA subunit are positioned to flank Asp32 of MotB, so that most of the conserved residues are in the channel. This arrangement also brings into proximity the pairs of positions that gave the highest yield of cross-linking between A4 and B (210−40 and 213−36), and between A3 and B (177−33 and 177−36).

Results of Trp-scanning mutational studies (*23*, *25*) are consistent with this arrangement of membrane segments (Figure 10C). While most Trp replacements in segment A3 or A4 eliminated motility, about half of the Trp replacements in A1 or A2 allowed motility, often as good as that of the wild type. This suggests that segments A1 and A2 are in more exterior, lipid-exposed locations. The angular orientations of the segments in Figure 10 are also consistent with the Trp-scanning results. In both A3 and A4, positions that tolerate Trp are on helix faces away from the channel lining. The Trp-tolerating face on A3 includes a well-conserved residue (Gly 179), and while Trp replacements in this segment allowed some motility, the swarming rates were significantly reduced (*23*). This face on A3 is evidently important for optimal function, possibly because it contacts segment A1 or A2. In MotB, Trp replacements in the inner half of the segment generally eliminated function, whereas most replacements in the outer half were tolerated (*25*). For the arrangement pictured (Figure 10C), the innermost positions in B that tolerated Trp are on faces away from the channel.

Trp replacements that prevented motor rotation showed varying levels of dominance when the mutant proteins were expressed in wild-type cells. The model predicts that most of the strongly dominant Trp replacements occur within or near the proton channels. This holds for replacements in B as well as in A3 and A4, and suggests that strong dominance might be the result of blocking the channels. The Trp replacements that eliminated motility but were less dominant are on faces away from the channels, where they might alter the packing between membrane segments. (While the Trp replacement at MotA residue 187 is recessive and predicted to be in the channel, that protein was found to be unstable (*23*).)

Some of the single-Cys-replacement mutants and several of the double-Cys mutants were nonfunctional. The high frequency of synergistic defects in the double mutants is consistent with any model (including that in Figure 10) in which segments A3, A4, and B are near each other and form a functionally important part of the complex. Further interpretation of the mutational effects will require more structural information. A possible concern is that some of the nonfunctional mutant proteins have an altered arrangement of membrane segments, so that cross-link yields do not reflect the normal arrangement. The important segment proximities are established by results from many double mutants, however, several of which gave a good cross-linking yield and were still functional. These include the A3/A4 mutants 178/210, 181/210, 178/213, and 178/214, the A3/B mutants 173/35, 174/ 36, 177/36, and 181/39, and the A4/B mutants 210/40 and 213/36.

Because polar residues are scarce in the membrane segments of MotA and MotB, it was suggested that the ion-conduction pathway might consist mainly of water molecules (*23*, *25*). In the model in Figure 10, the residues that line the channel are mostly small and aliphatic, with polar side chains occurring only at D32 and T35 in segment B, and T209 in segment A4. In the *E. coli* proteins, predicted channel-facing residues in the segments are P173, G176, A180, V184, and A187 in segment A3, I202, A205, G212, T209, and A216 in A4, and D32, T35, A36, A39, and V43 in segment B. These are residues in just the inner two-thirds of the segments; the channel must extend to the periplasm, but the segment arrangement near the outer ends is not yet well determined.

Certain residues in A3 and A4 are predicted to face each other across the channel (Figure 10). We did not see evidence of intrasubunit cross-linking between A3 and A4, even though such cross-linking would likely give a detectable mobility shift on gels (see, e.g., ref *13*). The absence of intrasubunit cross-linking could have a number of causes, but we note that it is consistent with an architecture in which segments A3 and A4 are held at some distance from each other to frame a pore occupied by water molecules.

Segments A1 and A2 presumably form another layer of helices around the outside of the complex, but we do not yet know their locations. Although the mutational results suggest that they are less critical for function than A3 or A4, segments A1 and/or A2 likely form the outer wall of the channel, and might also help to hold segments A3 and A4 in their correct relative positions.

The MotA/MotB complex is homologous to the ExbB/ExbD complex that functions in membrane transport, and to the TolQ/TolR complex that has a role in outer-membrane integrity (*2*, *26*, *27*). Patterns of sequence conservation, mutational results, and computational methods have been used to predict the arrangement of membrane segments in the ExbBD/TolQR/MotAB complexes (*27*, *28*). Like the model presented here, these models assigned the major channel-forming roles to segments A3, A4, and B (or the corresponding parts of the Exb/Tol proteins). The model of Zhai et al. is based on a 1:1 subunit composition and so is very different from the model proposed here. The model of Cascales et al. resembles our model in some essentials, having the same number of subunits in a similar overall arrangement. The arrangement proposed for the membrane segments is different from that in Figure 10, however, with the relative positions of segments A3 and A4 reversed, and the channels at different positions on the outside of the B dimer (*27*). While the Mot, Exb, and Tol complexes are clearly related, their structures may still differ in important ways, and a comparative analysis of these systems will

require better structural information on all three.

The occurrence of four MotA subunits in the complex is intriguing, particularly since the ion channels seem to be largely within MotA subunits rather than at the interfaces between subunits. In the model in Figure 10, two of the MotA subunits have no obvious, direct role in forming the channel. We believe that torque generation involves a conformational change in the stator complex, triggered by proton binding at Asp32 (*2*). The measured dependence of motor torque upon rotation speed is most consistent with a kinetic scheme in which the energy of two protons is used simultaneously to drive rotation (*29*). This finding, and the twin-channel architecture (Figure 10), suggests that two protons might act cooperatively to drive the conformational change. This would imply that the two Asp32 residues, although distant from each other in the complex, are functionally coupled. Allosteric enzymes typically have multiple subunits, and the MotA subunits that do not directly contribute to the channels might provide a physical connection that allows the channels to act cooperatively. Another possibility is that the MotA subunits exchange positions with each other as the complex undergoes cycles of protonation/deprotonation, so that each MotA subunit samples both (or all) of the environments in the complex. Yet another possibility is that proton flow causes the array of four MotA subunits to rotate continuously around the MotB dimer, rather than driving a reciprocating movement as envisioned before (*2*, *7*).

ACKNOWLEDGMENT

We thank J. S. Parkinson for strains, and Wallace Archer, Karen Jordan, and Nephi Thompson for assistance with pilot cross-linking experiments.

REFERENCES

1. Kojima, S., and Blair, D. F. (2003) *Biochemistry 42* , 26−34.
2. Kojima, S., and Blair, D. F. (2001) *Biochemistry 40*, 13041−13050.
3. Dean, G. E., Macnab, R. M., Stader, J., Matsumura, P., and Burke, C. (1984) *J. Bacteriol. 143*, 991−999.
4. Zhou, J., Fazzio, R. T., and Blair, D. F. (1995) *J. Mol. Biol. 251*, 237−242.
5. Zhou, J., and Blair, D. F. (1997) *J. Mol. Biol. 273*, 428−439.
6. Zhou, J., Lloyd, S. A., and Blair, D. F. (1998) *Proc. Natl. Acad. Sci. U.S.A. 95*, 6436−6441.
7. Braun, T. F., Poulson, S., Gully, J. B., Empey, J. C., Van Way, S., Putnam, A., and Blair, D. F. (1999) *J. Bacteriol. 181*, 3542−3551.
8. Stader, J., Matsumura, P., Vacante, D., Dean, G. E., and Macnab, R. M. (1986) *J. Bacteriol. 166*, 244−252.
9. Chun, S. Y., and Parkinson, J. S. (1988) *Science 239*, 276−278.
10. DeMot, R., and Vanderleyden, J. (1994) *Mol. Microbiol. 12*, 333−334.
11. Falke, J. J., and Koshland, D. E. J. (1987) *Science 237*, 1596−600.
12. Falke, J. J., Dernburg, A. F., Sternberg, D. A., Zalkin, N., Milligan, D. L., and Koshland, D. E. J. (1988) *J. Biol. Chem. 263*, 14850−58.
13. Pakula, A., and Simon, M. I. (1992) *Proc. Natl. Acad. Sci. U.S.A. 89*, 4144−48.
14. Lee, G. F., Burrows, G. G., Lebert, M. R., and Dutton, D. P. (1994) *J. Biol. Chem. 269*, 29920−29927.
15. Nagy, J. K., Lau, F. W., Bowie, J. U., and Sanders, C. R. (2000) *Biochemistry 39*, 4154−4164.
16. Jones, P. C., Jiang, W., and Fillingame, R. H. (1998) *J. Biol. Chem. 273*, 17178−17185.
17. Wolin, C. D., and Kaback, H. R. (2000) *Biochemistry 39*, 6130−6135.
18. Braun, T. F., and Blair, D. F. (2001) *Biochemistry 40*, 13051−13059.
19. Studier, F. W., and Moffatt, B. A. (1986) *J. Mol. Biol. 189*, 113−130.
20. Tang, H., Braun, T. F., and Blair, D. F. (1996) *J. Mol. Biol. 261*, 209−221.
21. Togashi, F., Yamaguchi, S., Kihara, S. M., Aizawa, S.-I., and Macnab, R. M. (1997) *J. Bacteriol. 179*, 2994−3003.
22. Blair, D. F., and Berg, H. C. (1991) *J. Mol. Biol. 221*, 1433−1442.
23. Sharp, L. L., Zhou, J., and Blair, D. F. (1995) *Proc. Natl. Acad. Sci. U.S.A. 92*, 7946−7950.
24. Sato, K., and Homma, M. (2000) *J. Biol. Chem. 275*, 5718−5722.
25. Sharp, L. L., Zhou, J., and Blair, D. F. (1995) *Biochemistry 34*, 9166−9171.
26. Saier, J., M. H. (2000) *Microbiol. Mol. Biol. Rev. 64*, 354−411.
27. Cascales, E., Lloubes, R., and Sturgis, J. N. (2001) *Mol. Microbiol. 42*, 795−807.
28. Zhai, Y. F., Heijne, W., and Saier, J., M. H. (2003) *Biochim. Biophys. Acta 1614*, 201−210.
29. Berry, R. M., and Berg, H. C. (1999) *Biophys. J. 76*, 580−587.

BI035406D